OUT-OF-PLANE BEHAVIOUR OF FIBRE REINFORCED CEMENT COMPOSITE (FRCC) RENDERED DRY STACK CONCRETE MASONRY WALLS

M. DHANASEKAR[1] , W. HOLT[2], M. FEROZKHAN[3] AND R. DHANASEKAR[3]

[1] Professor, School of Urban Development, QUT, Brisbane 4001, Australia.
[2] Principal Engineering Manager, Hanson Masonry, Brisbane 4207, Australia.
[3] PG Student CRE, CQU, Rockhampton 4702, Australia.
[4] Senior Lecturer, CQU, Rockhampton, 4702, Australia.

SUMMARY

A dry stack concrete masonry (DSCM) walling system rendered with fibre reinforced cement composite (FRCC) is addressed in this paper. Out-of-plane behaviour of this walling system due to lateral pressure loading was examined by fabricating and testing six full scale wall specimens. All walls were 1400mm high; two of them were 900mm long and the remaining four were 1800mm long. The walls spanned such that they either were subjected to vertical or horizontal bending. The failure mode, moment capacity in horizontal and vertical bending, the ultimate pressure loading and the load-deflection behaviour of the walls are described.

INTRODUCTION

Masonry walls are vulnerable to out-of-plane bending. As dry stack concrete masonry (DSCM) walls contain no mortar either in the bed joint or in the perpend joint, the dry stacked blocks are expected to rotate relative to each other during out-of-plane bending in a complex manner with the assistance of friction between the units. To impart the tensile strength necessary to resist out-of-plane pressure loading and to prevent ingress of rain water to the interior, DSCM walls are rendered with fibre reinforced cement composite (FRCC). The behaviour of DSCM walls rendered with FRCC under out-of-plane bending evaluated from experimental investigation is reported in this paper. The ultimate bending capacity and the deformation behaviour of the DSCM walls are described and discussed. Six composite walls made from blocks wrapped with the FRCC were constructed and cured within an environment controlled room (ECR) where the temperature and humidity were maintained at $20^{\circ}C \pm 3^{\circ}C$ and $60\% \pm 5\%$ respectively to ensure minimal variability in FRCC. These walls were subjected to lateral pressure loading and tested in two series of three walls each. Strains were measured on the tension face of each wall and the deflections were recorded for the walls tested in the second series. The walls exhibited highly improved out-of-plane bending capacity due to FRCC rendering associated with sudden noisy failure. However, after failure the wall as a whole and the dry stack blocks remained contained within the FRCC wrapping.

LITERATURE REVIEW

Dry stack masonry is not a new concept; therefore, a comprehensive review is beyond the scope of this paper. Only papers relevant to the experimental testing of dry stack walls are reviewed.

Most of the relevant papers cover seismic retrofitting using factory made fibre composite tapes. As such no paper was found on walls that are built with site manufactured FRCC rendering.

Early work of Hamid et al (1993) and the most recent work of Mosallam (2007) consistently illustrate the enormous gain in capacity associated with reduced ductility/ brittle failure of masonry walls. Ehsani and Saadatmanesh (1996), however, reported improved ductility of un-reinforced masonry (URM) walls retrofitted with fibre composites on tension side only based on testing of six walls. Griffith et all (2001, 2004) reported static and dynamic test data of full scale unreinforced/ un-retrofitted clay brick masonry walls and concluded that the masonry walls could be designed using displacement based philosophies. Hamoush et al (2002) reported data from 18 walls tested under out-of-plane displacement controlled line loading. Air bags were used in the testing of walls by Ehsani and Saadamanesh (1996), Griffith et al (2001), Hamilton and Dolan (2001), and Mosallam (2007).

EXPERIMENTAL INVESTIGATION

Seven course hollow block composite walls of 150mm gross thickness as shown in Figure 1 were constructed and tested in the heavy testing laboratory (HTL) of the Central Queensland University.

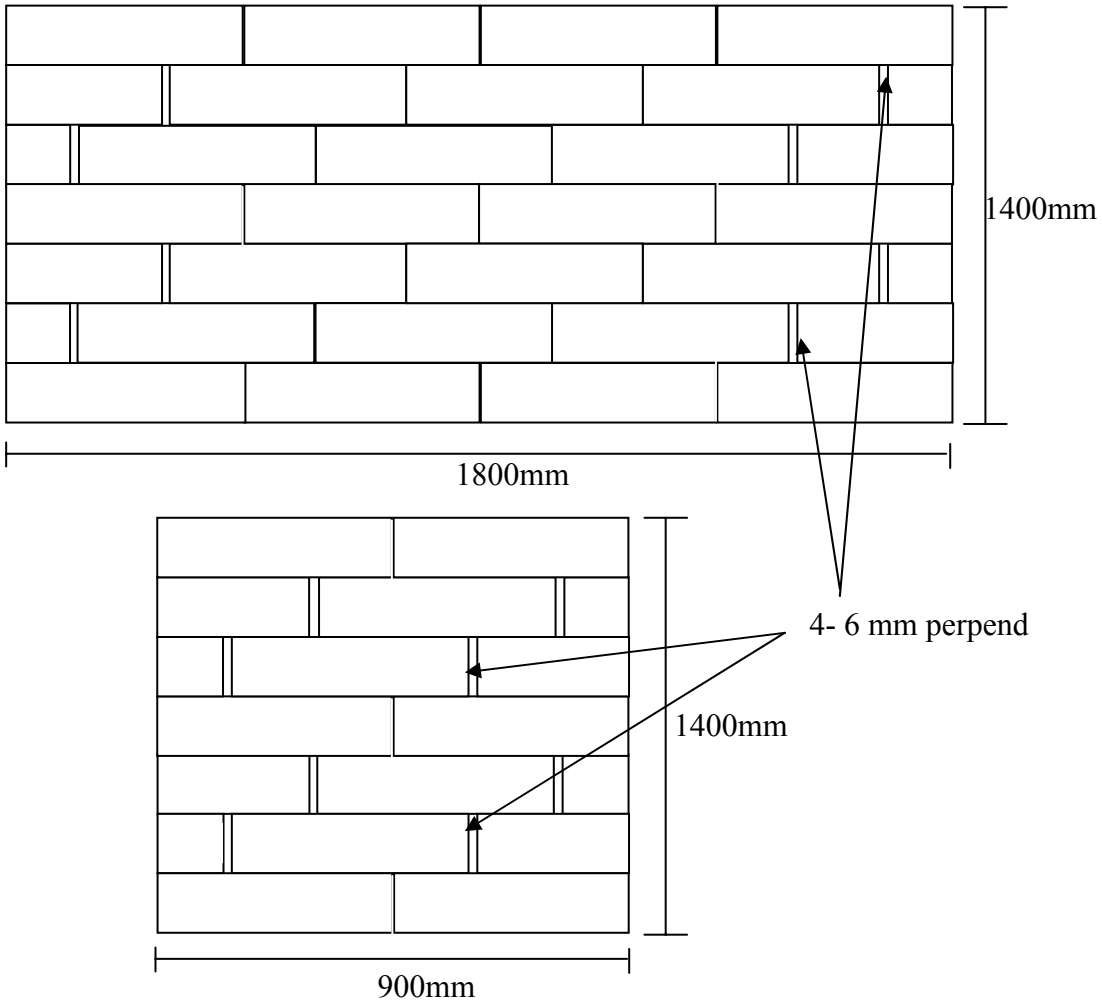

Figure 1. Configuration of DSCM Walls

The top, middle and bottom courses of the walls contained only full blocks. All other courses contained combinations of other blocks. All walls were wrapped with 5 mm thick FRCC, thus the nominal thickness of the walls was 160 mm. Walls were constructed by a professional tradesman on a 5mm layer of fibre reinforced cement polymer matrix sandwiched with a fibre mesh. The base course was laid followed by stacking of the full wall as per Figure 1. The FRCC wrapping was then completed all around the wall. A dry stacked wall prior to and during rendering is shown in Figure 2. All walls were constructed over visqueen plastic sheets on a specially fabricated trolley so that the walls could be moved around and out of the ECR easily from where they were transported to the testing lab by fork lift.

All walls were of constant height to thickness ratio of 8.8 but of varying length. A minimum of two specimens was constructed for each category.

Figure 2. DSCM wall construction stages

Instrumentation

Five linear variable differential transducers (LVDTs) and three strain gauges were used to measure the deflections and surface strains of the walls. All these instruments were fitted to one face of the wall as the opposite face of the wall was subjected to fluid pressure. One LVDT was positioned exactly at the mid point of the wall. Four other LVDTs were then positioned equidistant from the central LVDT. For this purpose, the positions of the four LVDTs were marked off as 1/3 distance from the closest edge of the wall. Two of the three strain gauges were fixed parallel to the bending direction at 1/3 span and the third at the mid point of the wall. An independent mounting frame to hold the LVDTs with adjustable length was specially fabricated. Deflections were measured on walls tested in the second series only.

Testing Program

The specimens were carefully laid horizontally for loading as shown in Figure 3. The walls were tested as slabs supported on two opposite edges. The walls are designated “CW” denoting composite wall with the first suffix corresponding to the test specimen number (1, 2 or 3) and the second suffix denoting the testing series (1 or 2). Both first and second series of specimens (walls CW_{11},CW_{21} & CW_{31} and CW_{12},CW_{22} & CW_{32}) were tested for ultimate capacity and strains. Deflection measurements were made only on the walls tested in the second series (walls CW_{12},CW_{22} & CW_{32}).

The DSCM walls considered in this paper were expected to fail at pressures in excess of 50 kPa. Therefore a heavy duty bag capable of generating a fluid pressure of more than 70 kPa under constrained conditions was developed with the help of Beehive Vinyl Products Pty Ltd,

Townsville, Australia. The bag was constrained between the wall and the strong floor as shown in Figure 3. Two separate pressure bags were used to test the three walls. In its inflated state, the bags measured $1500 \times 1200 \times 170$ mm (for testing walls CW_{11},CW_{12} and CW_{21} CW_{22}) and $1200 \times 600 \times 170$ mm (for testing walls CW_{31} and CW_{32}).

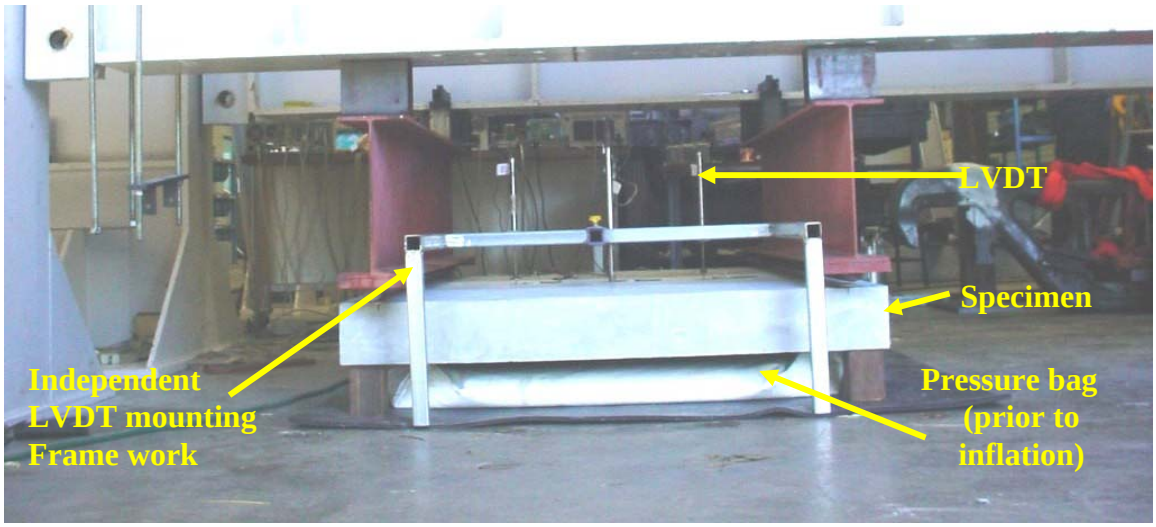

Figure 3. Arrangement of Instrumentation

The loading arrangement utilised a pair of 410 UB "I" sections of 2000 mm long for providing reaction to the wall. The support beams 410 UB were in turn connected to the beams of two portal frames arranged parallel to each other. When the air bag was pressurised, the wall moved up and reacted to the 410 UB beam through 50mm diameter rollers and 4mm thick plywood strips. Once the compressed fluid pressure inside the bag equaled the weight of the wall (approximately 4 kPa), the wall started floating and the rollers and the plywood were positioned appropriately. The temporary wooden support blocks were removed once the wall attained the static equilibrium balancing self weight as desired. The data acquisition system was zeroed corresponding to this pressure to enable the direct measurement of the pressure required to fail the wall (excluding the self weight of the wall). The rollers allowed the wall to rotate freely at the support and the plywood strips prevented application of concentrated load and subsequent localised bearing failure. The pressure was increased further monotonically at a rate of approximately 5 kPa / min. The pressure versus mid span deflection was monitored live during the test. The data were analysed carefully and any noise filtered out. The mode of failure, the deformation behaviour and the ultimate load carrying capacity of the walls tested are discussed in the ensuing sections.

Mode of Failure

All specimens exhibited cracking at approximately 40 % - 50 % of the ultimate load at the top surface (tension face) of the FRCC. All specimens failed with a noisy explosion at ultimate. All walls failed due to a single major crack formed in the region of maximum bending moment. The absence of a distributed array of cracks is typical of brittle un-reinforced structures.

The failure path of CW_{11} & CW_{12} specimens appeared to have been affected by the bed and perpend interfaces between blocks as evidenced by the zigzag pattern in the crack path as

shown in Figure 4. This type of failure is similar to those of a conventional masonry walls subjected to horizontal bending.

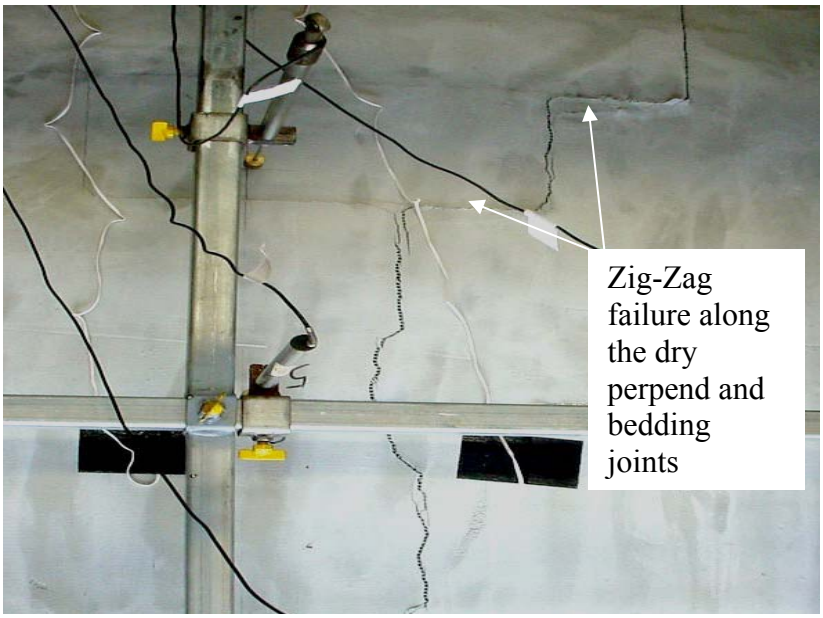

Figure 4. Failure pattern of CW_1 wall specimens

Walls CW_{21}, CW_{22} and CW_{31}, CW_{32} failed along the bed joint in the vicinity of the maximum bending region with a single straight crack that is typical of vertical bending as shown in Figures 5 and 6. In-spite of the noisy failure, all the individual blocks of the wall specimen were intact and it was easy to transport the failed walls to the storage yard. The composite wrapping provided the necessary integrity.

The maximum peak load recorded was 55 kPa for CW_{32} and the maximum mid span deflection was 9 mm for CW_{22}. All walls exhibited evidence of tensile splitting of fibre mesh in the tension side.

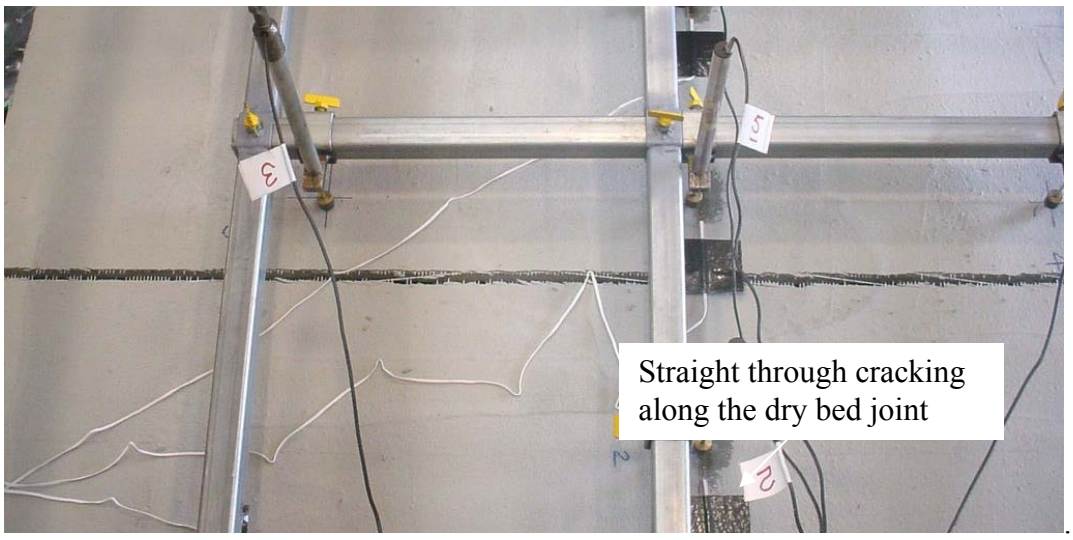

Figure 5. Failure pattern of CW_2 wall specimens

Figure 6. Failure pattern of CW_3 wall specimens

Behaviour of DSCM composite wall

The failure of walls tested is presented in Table 1. The specimen configuration, failure load and equivalent load and the mean equivalent load and failure pattern are shown in columns 1-6. As the pressure bag did not occupy the full length of wall, the ultimate uniformly distributed pressure (W_u) recorded in each case was converted to an equivalent pressure (W_{ue}) using Eq. 1.

$$W_{ue} = W_u \times \frac{L_b}{L_w} \quad (1)$$

in which L_b and L_w are the lengths of bag and composite wall respectively.

Table 1 DSCM composite wall -Experimental failure details

Designation	Size span×length (mm × mm) & Bending Direction	Failure Load W_u (kPa)	Equivalent Uniformly distributed load (EUDL) W_{ue} (kPa)	Mean EUDL W_{ue} (kPa)	Crack Pattern
CW_{11}	1490×1410 Horizontal Bending	24	20.4	21.3	Zigzag cracking along the dry perpends and bed -typical of horizontal bending
CW_{12}		26	22.2		
CW_{21}	1200×1800 Vertical Bending	38	31.7	29.2	Straight line cracking along the dry bedding joints- typical of vertical bending
CW_{22}		32	26.7		
CW_{31}	1200×900 Vertical Bending	54	36.0	36.3	
CW_{32}		55	36.7		

On a minor note, it is worth explaining the rationale of testing two walls in each series under vertical bending and only one wall in each series in horizontal bending. At a first glance it would appear that the horizontal bending that exhibit zig-zag failure path actually requires more specimens testing rather than the straight crack failure of vertical bending. The problem we had that lead to the decision of testing two lengths of vertical bending walls in each series was associated with the pressure bag sizes that are very special and carefully fabricated from standard size fabric with the objective of minimising stiches. This has resulted in none of the bags actually be able to cover the full length of the walls, thus creating a two dimensional effect of loading. We tested two vertical bending specimens in each series, precisely to eliminate any confusion on the validity of results based on loaded area as these specimens must fail in a straight line fashion.

Both walls tested for each category failed at fairly consistent pressure levels (with variation in the range of 2% to 19%). These pressure levels are much higher than that for the un-wrapped/ unreinforced masonry walls. For example, as per AS3700 Cl. 7.4.2, had the walls failed under vertical bending and been built using traditional unreinforced masonry, the pressure load at failure would have been only 2.5kPa (as against the experimental mean values of 29.2kPa and 36.3kPa). The 2.5kPa capacity was based on an assumed flexural tensile strength of 0.2MPa. Another way of looking at the result is to examine the capacity of dry stack masonry without the FRCC wrapping. In the absence of the FRCC wrapping, the dry stacked masonry would have collapsed under a pressure of only 0.20kPa due to vertical bending as per AS3700 Cl. 7.4.2. For this calculation the flexural tensile strength was assumed nil with the capacity derived entirely from the self weight of the wall at mid span. The benefit of FRCC wrapping is thus obvious.

The moment capacity of the wall was calculated using the basic strength of components as shown in Table 2 (columns 2 and 3). The experimentally determined moment capacity is also presented in the Table 2 (column 4). The moment capacity was calculated using the tensile strength of FRCC as 5.8 MPa and the thickness of FRCC in tensile zones as 2.5 mm. The lever arm (distance between compression and tension forces) was 134.7 mm when the compression face shell was included, whilst the lever arm was 147.9 mm when the compression face shell was excluded. In Figure 7 the lever arm (j_d) calculation for inclusion of the compression face shell is illustrated. The breadth and thickness of the compression and tension FRCC layers are (B_1, t_1) and (B_2, t_2) respectively and that of the concrete face shell are (B_3, t_3). Here $B_1 = B_2 = B_3$. D is the total depth, d_n is the depth to neutral axis, de is the effective depth; C (= C_1 +C_2) is compressive force and T is tensile force. C_1 and C_2 are the compressive force resisted by FRCC and face shell respectively.

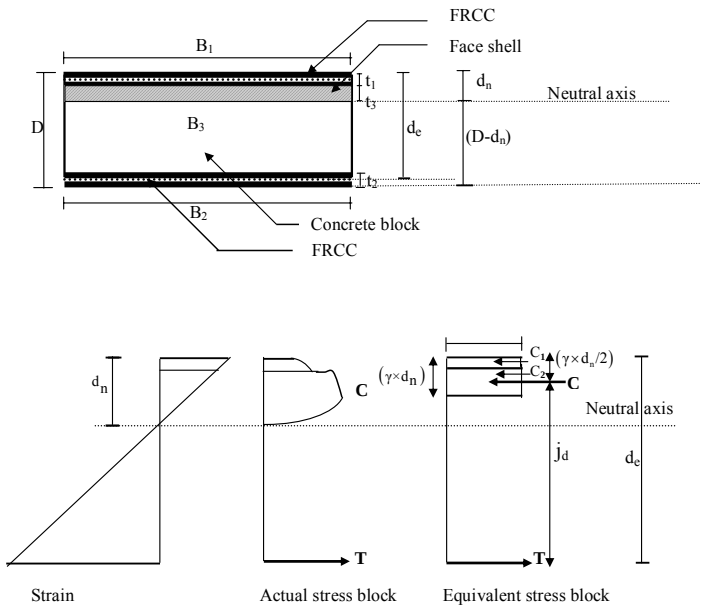

Figure 7. Calculation of Moment Capacity

Table 2 DSCM composite wall –Moment capacity

Specimen Identification	Moment capacity (kNm)		
	Calculated including compression face shell	Calculated excluding compression face shell	Experimental (Mean) M_{max}
CW_{11} & CW_{12}	3.03	2.75	5.90
CW_{21} & CW_{22}	3.86	3.52	5.25
CW_{31} & CW_{32}	1.93	1.76	6.55

The data show that the calculated moment capacity is significantly lower than that of the experimental prediction. Although from a practical perspective it is desirable to have the calculations providing conservative values related to experimental prediction, the considerable deviations between the calculated and experimental values requires explanation, which may be stated as follows:

The FRCC tension coupon tests have predicted maximum strain value of 1460 microstrain under direct tension and only 800 microstrain under flexural tests with the FRCC specimens exhibiting complex fibre pull out mechanism of failure (with no fibre fracture). A typical plot of the equivalent load versus mid span longitudinal strain for walls CW_{11} is shown in Figure 8. From the graph shown in Figure 8, it can be observed that the FRCC in the tension face of the wall undergoes to maximum strain of approximately 5000 microstrain. This shows that when one of the faces of the FRCC is provided with a base restraint (shells of the block), the FRCC elongates much more relative to the un-supported direct tension test where it failed approximately at a maximum strain of 1460 microstrain. Thus to determine the true behaviour of the FRCC in walls, perhaps one must test specimens restrained by block face shells.

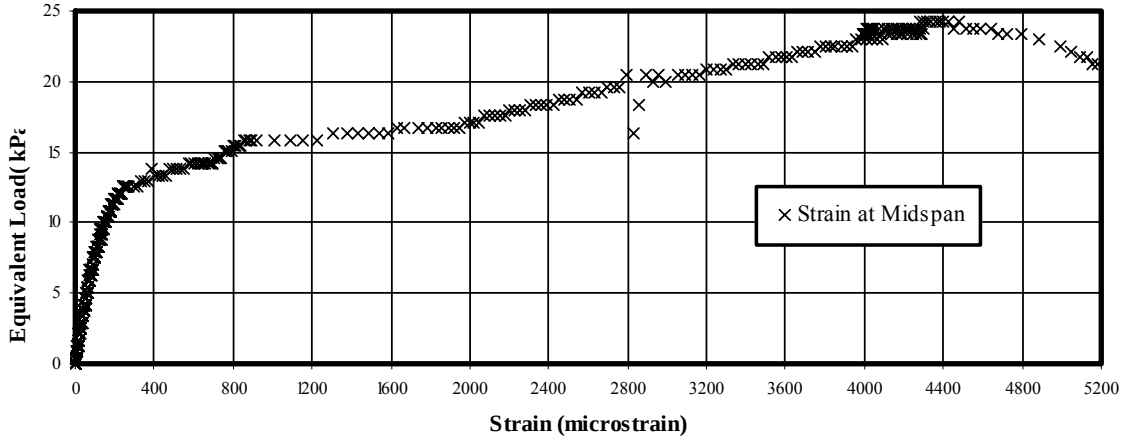

Figure 8. Variation of Longitudinal Strain in CW_{11}

Load –Deflection relationship

Deformations of three walls tested in the second series were recorded. The observed displacement at the mid span of the wall is plotted against the equivalent load in Figure 9. The

load deflection curves exhibit significant nonlinearity from the early stages of loading. As the walls failed suddenly, no meaningful post-peak load information could be recorded.

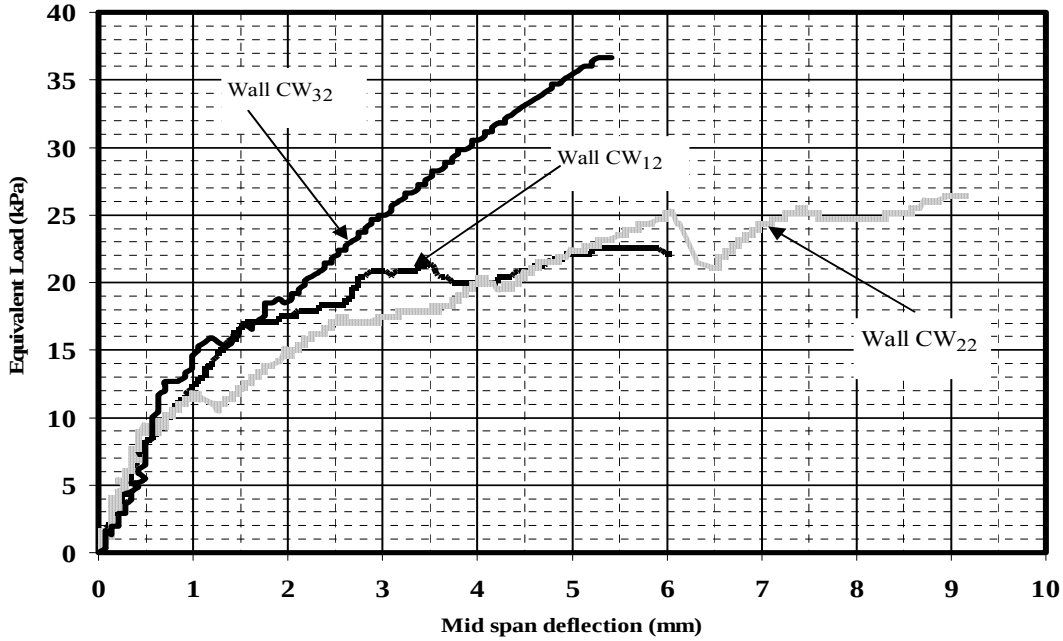

Figure 9. Experimental Load - Deflection Curves

SUMMARY AND DISCUSSIONS

This paper has reported testing of six DSCM walls subjected to one way out-of-plane bending. Both horizontal and vertical bending behaviour were investigated. The theoretical bending capacities calculated were compared with the experimental values of the failure load.

The walls were constructed in an environmental control room (ECR), where the temperature and humidity were maintained at $20^{\circ}C \pm 3^{\circ}C$ and $60\% \pm 5\%$ respectively.

Six walls (three each of two series) were tested under out-of-plane loading. Loading was applied using fluid pressure. Maximum failure pressure obtained in the test series was 55kPa. One wall was tested to simulate horizontal bending and the other two walls were tested to simulate vertical bending. The walls failed under horizontal bending showed evidence of some limited zigzag crack path. The walls under vertical bending failed along the bed joint exhibiting a single, straight crack. Only one dominant crack was noticed in each wall. Although each failure was noisy, the walls maintained their integrity and remained as a unit and were easy to handle. Deformation measurements taken from the walls tested in the second series exhibited marked non-linearity.

The bending capacity of the walls could not be predicted from the strength properties of the constituents (FRCC and block). The following perhaps explain the reasons for this failure. Strain measurement in walls tested under horizontal bending exhibited ultimate strain values of approximately 5000 microstrain. None of the tension specimens (direct or flexural) of FRCC exhibited such high strain values; the maximum ultimate strain being 1460 microstrain. Prediction of ultimate bending capacity showed much lower values compared to the

experimental value. It was therefore concluded that FRCC in the structure behaved different to the simple material testing; support on one face of the FRCC appeared to have positively contributed to the behaviour of DSCM wall under tension.

In conclusion it could be stated that the DSCM system examined in this paper possess very good flexural capacity, more than adequate normally required for the cyclonic regions of Australia. The failure is, however, noisy and sudden indicating lack of ductility. Further research is needed to improve ductility.

To minimise the variability in test results and to obtain consistency between specimens tested, all walls were cured in the ECR, although this is not representative of the field practice. This matter requires further examination. The actual effect of curing on full-scale structural walls could not be correlated to the variability obtained from the material testing. This is especially so due to one of the findings that the *material test data could not accurately predict the strength of the walls*.

It is recommended to

- Devise careful experimentation to examine the behaviour of the FRCC composite wrapping material to strain levels of up to 5000 microstrain.
- Develop a first principle mechanics approach for the determination of the bending capacity of the DSCM wall system to account for two way bending.
- Develop an appropriate method of testing the DSCM wall system under two way bending.

REFERENCES:

1. Ehsani, M. and Saadatmanesh, H. (1996), "Seismic Retrofit of URM Walls with Fiber Composites", *TMS*, vol. 14, no. 2**,** pp. 63-71.
2. Griffith, M.C., Lam, N.T.K., Wilson, J.L. and Doherty, K. (2004), Experimental Investigation of Unreinforced Brick Masonry Walls in Flexure", J of Struct Engg., ASCE, Vol. 130, No. 3, pp. 423-432.
3. Griffith, M. C., Willis, C. R. and Lawrence, S. J. (2001), "Flexural Behaviour and Design of Unreinforced (Brick) Masonry Walls", *Proceedings of the 6th Australasian Masonry Conference,* Adelaide, Australia, pp. pp 177, 179, 183.
4. Hamid, A., Larralde, J. and Salama, A. (1993), "Properties of Hollow Concrete Masonry Reinforced with Fiberglass Composite", *ACI Special Technical Publication SP-138*, pp. pp 465-476.
5. Hamilton, H. R. and Dolan, C. W. (2001), "Flexural Capacity of Glass FRP Strengthened Concrete Masonry Walls", *Composites for construction*, vol. 5, no. 3**,** pp. 171,173, 177.
6. Hamoush, S. A., McGinley, M. W., Mlakar, P. and Terro, M. J. (2002), "Out-of-Plane Behaviour of Surface-Reinforced Masonry Walls", *Journal of Construction and Building materials*, vol. 16, no. 6**,** p. 341-351.
7. Mosallam, A.S. (2007) "Out-of-Plane Flexural Behaviour of Unreinforced Red Brick Walls Strengthened with FRP Composites", *Composites Part B: Engineering*, Vol. 38, pp559-574.